ORIGINAL PAPER

Kinetics, isotherms and thermodynamics of oil spills removal by novel amphiphilic Chitosan-*g*-Octanal Schiff base polymer developed by click grafting technique

Bassant Yousry Eweida[1] · Ahmed Mohamed Omer[2] · Tamer Mahmoud Tamer[2] ·
Hesham Abd-Elfatah Mohamed Soliman[3] · Ahmed Amin Zaatot[4] ·
Mohamed Samir Mohy-Eldin[2]

Abstract

Kinetic, isothermal and thermodynamic studies for the oil spills removal process have been conducted by Chitosan and novel amphiphilic Chitosan-g-Octanal Schiff base adsorbents developed by click chemistry and evaluated successfully in the removal of heavy crude oil spills. Chitosan was first prepared from wastes of marine shrimp shells, and then Chitosan and Chitosan-g-Octanal Schiff base adsorbents were synthesized and verified their structures, thermal stability and their morphological changes using FT-IR spectroscopy, TGA and SEM. The oil adsorption percentages (%) using heavy crude oil were 96.41% for the Chitosan-g-Octanal Schiff base adsorbent compared to 64.99% for native Chitosan counterpart. High rate of adsorption was observed where 40% of oil adsorbed within 15 min only using the Chitosan-g-Octanal Schiff base adsorbent compared to 90 min for native Chitosan adsorbent. The adsorption process followed the pseudo-second order model, and the equilibrium data were sufficiently fitted with the Langmuir model with a maximum adsorption capacity 30.30 g/g at 25 °C. Thermodynamic parameters computed from Van't Hoff plot confirmed the process to be endothermic, favorable and spontaneous.

Keywords Chitosan · Schiff base · Octanal · Click grafting · Hydrophobic characters · Oil spill removal · Kinetics · Isotherms · Thermodynamic studies

✉ Mohamed Samir Mohy-Eldin
mmohyeldin@srtacity.sci.eg

Extended author information available on the last page of the article

Introduction

Water is a very important constituent of the ecosystem on the Earth and essential component of life. The demand of water is increasing day by day due to an increase in population and in living standard. The quality of our water resources is deteriorating day by day due to the continuous addition of undesirable chemicals in them. Various water pollutants, such as metal ions, the residues of the drugs and pharmaceuticals (new emerging pollutants), dyes, Chiral pollutants and pesticides in water, are hazardous. Since these pollutants are very dangerous and have a direct and indirect impact on the human health life and the surrounding environment, many reviews and studies about have been published [1–5].

The different methods have been developed and used for water treatment. These methods include filtration, screening, oxidation, precipitation, coagulation, centrifugation, flotation, crystallization, sedimentation, distillation, evaporation, reverse osmosis, electrochemical, ion exchange, adsorption, etc. Among them, adsorption phenomenon is considered as one of the appropriate water treatment methodologies because of its ease of operation and the accessibility with a wide range of adsorbents for the removal of different pollutants [6–16].

When oil is explored, transported and stored and its derivatives are used, there is risk for spillage with the potential to cause significant environmental impact [17]. Due to its destructive properties, the entire character of the area is damaged once an area has been contaminated with oil. In addition, when oil encounters something to cling to (e.g., beach, rocks, feathers of a duck or a bathers hair), it is difficult to remove [18]. Therefore, pollution by petroleum oils affects sea life, economy, tourism and leisure activities due to the coating properties of these materials [17].When oil is spilled in water or on land, the physical and chemical properties of oil change progressively. The spilled oil contributes an undesirable taste and odor to drinking water and causes severe environmental damage [19]. Oil pollution from food production, catering industry, petroleum chemical and petroleum mining has drawn extensive attention of many researchers in recent years. Many methods, such as mechanical extraction, in situ combustion and chemical degradation, have been used to the cleanup of oil from polluted areas. Owing to better economical and environmental benefits, the use of sorbent is considered as an effective method to concentrate, transfer and absorb spilled oil [20]. High-efficient oil sorbent is required to possess desirable characteristics, such as excellent hydrophobicity and oleophilicity, high uptake capacity and fast oil sorption rate, low water uptake and insolubility, low cost and high buoyancy. So far, various materials including natural materials such as seaweed, alginate, dead biomass, rice hulls, carrageenan, lignins, cellulose, chitin and chitosan [21], inorganic mineral materials [22] and organic synthetic fibers [23] have been used for oil sorption [24]. Chitosan, discovered by Rouget in 1859 [25], is a technologically important poly-saccharide biopolymer. Chemically, it is a high molecular weight linear polycationic hetero polysaccharide consisting of two monosaccharides, N-acetyl-D-glucosamine and D-glucosamine, linked together by β-(1→4) glycosidic bonds (Fig. 1). The relative amount of the two monosaccharides in Chitosan may vary,
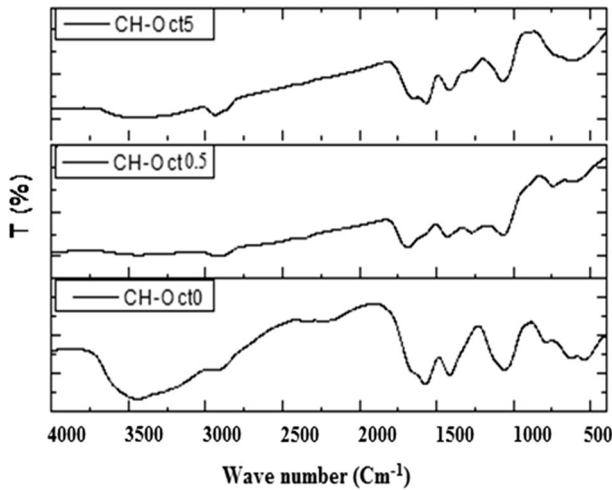
Fig. 1 FT-IR of Chitosan and Chitosan-g-Octanal Schiff base

giving samples of different degrees of deacetylation (75–99%), molecular weights (50–2000 kDa), viscosities, pKa values, etc. [26–28]. Therefore, the term Chitosan does not refer to a uniquely defined compound; it merely refers to a family of copolymers with various fractions of acetylated units.

Chitosan is the deacetylated derivative of Chitin, which is the second most important natural polymers on Earth after cellulose (Scheme 1), [28] distributes widely in nature and is mainly present as the structural component of crustacean shells [29].

Chitosan is also found in nature, such as in cell walls of fungi of the class *Zygomycetes*, in the green algae *Chlorella* sp., yeast and insect cuticles. Recent advances in fermentation technology suggest that the cultivation of fungi (*Aspergillus niger*)
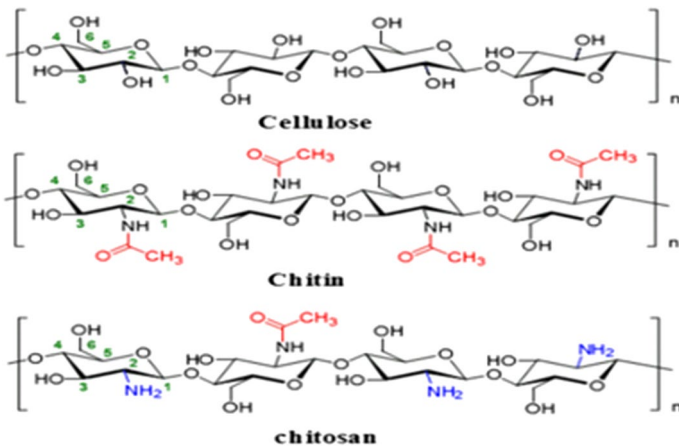
Scheme 1 Chemical structure of cellulose, Chitin and Chitosan

can provide an alternative source of Chitosan. However, Chitosan from both sources differs slightly: whereas the acetyl groups in Chitosan produced from crustacean Chitin are uniformly distributed along the polymer chain, a Chitosan of similar degree of deacetylation isolated from fungal cell walls would possess acetyl residues that are grouped into clusters [28, 30].

Indeed, Chitosan is becoming most popular in different applications due to its excellent unique properties such as bio-degradability, non-toxicity, lower density, ease modification and lower cost [31]. Furthermore, Chitosan can undergo physicochemical modification for allowing the formation of functional derivatives with a highly hydrophilic and/or hydrophobic character such as coating, carboxy methylation [32, 33], grafting and amination [34–36]. It was reported that Chitosan has various functional groups like hydroxyl and amino groups which induced simple chemical transformation and modifications. Schiff base compounds containing an imine group are usually formed by the condensation of a primary amine with an active carbonyl. The presence of amine groups in the polymeric chain leads to the possibility of a several chemical modifications, including the preparation of Schiff bases (–RC=N–) by reaction with aldehydes and ketones [37, 38]. Its attractiveness as analytical reagent rises from the fact that they enable simple and inexpensive determinations of various organic and inorganic substances [39]. It was reported that Chitosan has been used for the treatment of wastewater from phenolic compounds [39, 40] using immobilization of bacteria on Chitin and Chitosan flaked which degrade hydrocarbons. Additionally, Chitosan showed high adsorption capacity when it applied as oil adsorbent material for removing oil spills [28].

Different materials have been developed and used as sorbents for oil spills [41, 42]. For many reasons and advantages, nature-based sorbents are recommended [43]. However, drawbacks such as low hydrophobic character and limited oil sorption capacity compromised the wide application [44]. Many ideas have been investigated to overcome such drawbacks, such as induced lauric acid to the structure [45], grafting with acrylate polymers [46–48] and formation of Schiff bases [49]. Among natural-based materials, Chitosan comes in the lead for treating contaminated waters due to its reach structure with both hydroxyl and amine groups [50–54]. Many modification routes have been investigated to increase Chitosan applications, including the grafting technique [55–58].

In this study, kinetic, isothermal and thermodynamic studies for the oil spills removal process have been conducted by Chitosan and novel amphiphilic Chitosan-g-Octanal Schiff base adsorbents developed by click chemistry and evaluated successfully in the removal of heavy crude oil spills. The novel amphiphilic Chitosan-*g*-Octanal Schiff base oil adsorptive materials based on low-cost homemade Chitosan used click grafting technique between the aldehyde groups of Octanal and the Chitosan' amine groups. The developed Chitosan-*g*-Octanal Schiff base adsorbent acquire a higher hydrophobicity character relative to the Chitosan due to the hydrophobic character of Octanal and consuming the Chitosan' amine groups. Furthermore, other amine groups were engaged in the formation of three dimensions structure via crosslinking with glutaraldehyde. The crosslinking step reduces the hydrophilicity of the Chitosan backbone in addition to induce pores structure. Accordingly, the developed amphiphilic Chitosan-*g*-Octanal Schiff base can adsorb

oils through its hydrophobic Octanal grafted moieties from one hand and their pores on the other hand. The acquired hydrophobicity increases the affinity of the developed amphiphilic Chitosan-*g*-Octanal Schiff base towards the oils and decreases their affinity towards water. The novel materials were characterized using different characterization tools [28].

Experimental

Materials

Sodium hydroxide pellets were obtained from by EL. Pharanae Co. (Assay 99%, $M_{wt} = 40$ g/mol). **Acetic acid** (Purity 99.8%, $M_{wt} = 60.05$ g/mol), **glutaraldehyde** (GA; 99%) and octanal (Purity ≥ 95%, $M_{wt} = 130.23$ g/mol) were obtained from Sigma-Aldrich (Germany).**Ethanol** (Purity 99%), **hydrochloric acid** (Assay (37%)) and **ethyl alcohol absolute were** brought from El-Nasr Company (Alexandria). **Shrimp skeletons** were provided from commercial resource in Alexandria (Egypt). **Sodium chloride** and **sulfuric acid** (Purity 95–97%) were purchased from El-Gomhouria Co., (Egypt). **Crude oil sample:** Land Belayem (LB) was supplied from Belayem Petroleum Company (Table 1).

Methods

Chitosan preparation and purification

First, Chitin was extracted from crushed shells according to the published procedure [59]. The next step was the preparation of Chitosan from previously extracted Chitin via a simple de-acetylating process in an alkaline medium, which resulted in the removal of acetyl groups from the Chitin [60]**.** The resulted Chitosan was further purified according to the previous method [61]. The degree of de-acetylation was calculated using FT-IR, and potentiometric titration methods show very close results, 94.4% and 93.15%, respectively [62]**.**

Table 1 General characteristics of heavy crude oil	Property	LB(Heavy crude oil)
	Density gm/cm^3 at 20°c	0.9125
	Apigravity	23.5
	Viscosity at 100 °F cSt	482
	S. content %	3
	Asphaltenes %Wt	0.4

(a)
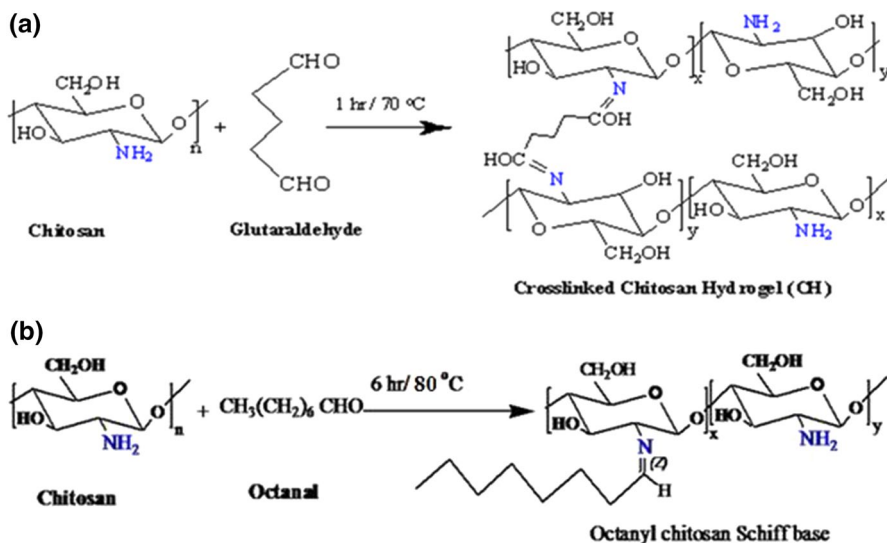
Scheme 2 Chitosan and Chitosan-g-Octanal Schiff base (Octanyl Chitosan Schiff base) adsorbents

Preparation of Chitosan-g-Octanal Schiff base

Chitosan primary amino groups react with active carbonyl groups of Octanal to produce the corresponding Schiff base as presented in Scheme 2. Previously purified Chitosan (0.4 g) was dissolved in 20 ml of 2% acetic acid and stirred at room temperature for 6 h. The resulting viscous solution was filtered through cheese cloth to remove un-dissolved particles and then added 10 ml ethanol to the viscous solution under stirring at room temperature; then, 5 ml of ethanol containing definite amount of Octanal was added to solution under stirring to have homogenous solution. This mixture was stirred for 6 h at 80 °C. The formation of gel refers to formation of the Chitosan-g-Octanal Schiff base. Then 100 μl of glutardehyde was added to the resulting product for 1 h at 80 °C. The resulting product was added to excess of 1 M sodium hydroxide solution. The precipitate was filtered and washed with distilled water and ethanol several times to remove un-reacted Octanal. The product was filtered and dried in a vacuum oven at 60 °C overnight. One mole of Chitosan click reacted with two different Octanal concentrations, namely 0.51 and 5.06 mol, and the prepared samples were coded as CH-Oct0.5 (38.25 G%) and CH-Oct5 (81.75 G%), while the Chitosan was coded as CH-Oct0 (0.0 G%).

The grafting percentage of Octanal was calculated according to the following equation [28]:

$$GP(\%) = [(W_1 - W_0)/W_0] \times 100 \qquad (1)$$

The W_0 and W_1 are the weights of Chitosan and the resultant Chitosan-g-Octanal Schiff base.

For the preparation of Chitosan adsorbent, the same procedure mentioned above was applied except for the skip of the Octanal addition step.

Material characterization

Physicochemical characterization

Infrared spectroscopic analysis (FTIR) The Chitosan and Chitosan-g-Octanal Schiff base structures were investigated by FTIR spectroscopic analyses using Fourier transform infrared spectrophotometer (Shimadzu FTIR—8400 S, Japan). Samples (2–10 mg) were mixed thoroughly with KBr, and the absorbance of samples was scanned from 500 to 4000 cm^{-1}.

Thermal gravimetric analysis (TGA) Analysis by TGA of samples was carried out using a thermogravimetric analyzer (Shimadzu TGA –50, Japan) under Nitrogen, at a gas flow rate of 20 mL/min, to evidence changes in structure as a result of the modification. In addition, samples were measured their weight loss starting from room temperature to 800 °C at a heating rate of 10 °C/minute.

Scanning electron microscopic analysis (SEM) Samples were fixed on aluminum stubs and vacuum-coated with gold before being examined by scanning electron microscopy. Morphological changes of the sample's surface were followed using a secondary electron detector of SEM (Joel JSM 6360LA, Japan). Two magnifications factors were used: 1000X and 5000X under 20 keV.

Determination of ion exchange capacity

A known weight of Chitosan or Chitosan-g-Octanal (0.1 g) was added to known volume of 0.1 M H_2SO_4 solution (20 mL) and the mixture was kept aside for 2 h. The mixture was filtered, and an aliquot was titrated against standard solution of NaOH. Similarly, control titration without the addition of Chitosan was also run. From the difference in the volume of NaOH required for neutralization, ionic capacity of Chitosan samples were calculated using the following equation:

$$Ion\ exchange\ capacity\ =\ \left(V_2 - V_1\right) a\ /\ w\ (meq/g) \tag{2}$$

where V_2 and V_1 are the volumes of NaOH required for complete neutralization of H_2SO_4 in the absence and presence of Chitosan, respectively. a is the normality of NaOH, and w is the weight of sample taken for analysis.

Water uptake

Water uptake estimation was performed by placing a weighed sample in 10 ml water. After 6 h the sample was then filtered off, carefully bolted with a filter paper and weighed. The water uptake was calculated by applying the following equation:

$$\text{Water uptake} \ = \ \left[\left(M - M_o \right) / M_o \right] \tag{3}$$

where M is the weight of the swelled sample at time t and M_0 is the weight of the dry sample [63, 64].

Oil uptake

Oil uptake was calculated by soaking a known weight of the samples (0.05 g) in 10 ml of oil (mineral oil, diesel oil, kerosene oil) and then placed in a closed glass containers for different time intervals, carefully bolted with a filter paper and weighed immediately in a closed balance. Oil uptake can be expressed by the following equation:

$$\text{Oil uptake} \ = \ \left[\left(W_t - W_o \right) / W_o \right] \tag{4}$$

where W_t is the weight of the soaked sample in the oil for certain time and w_0 is the sample initial dry weight [63, 64].

Results and discussion

Physicochemical characterization

The ion exchange capacity and the water uptake of Chitosan and Chitosan-g-Octanal Schiff base adsorbents have been measured. The measured values were found 9.9, 6.0 and 1.47 (meq/g) of CH-Oct0, CH-Oct0.5 and CH-Oct5 adsorbents, respectively. These findings refer to consumption of the Chitosan amine groups in the formation of Schiff base via click reaction with Octanal aldehyde groups. The same trend was observed when Chitosan reacts with aldehydes and ketons [65].

On the other hand, it was clear a gradual decrease of the water sorption capacity of CH-Oct0, from 3.4, to 2.75, and 0.0 (g/g) of the CH-Oct0.5 and CH-Oct5 samples. The click reaction of Octanal with Chitosan free amine groups replaced the hydrophilic amine group with an alternative hydrophobic aromatic one. The same results were observed by Mohy Eldin et al.[28, 38–40, 63].

High-efficient oil sorbent is required to possess desirable characteristics, among them, excellent hydrophobicity and low water uptake and solubility [4]. The range of working pH was widened at which Chitosan adsorbents kept low solubility and water uptake increase its potential as oil spills adsorbent. Amine groups of Chitosan have an essential role in Chitosan solubility. The protonation of amine groups of Chitosan in the acid medium enhances Chitosan solubility. Sogias et al. [66] explored the factors affecting the solubility of Chitosan in Water. Due to its semicrystalline nature, derived mainly from inter- and intramolecular hydrogen bonds, Chitosan is water-soluble only at pH < 6. In acidic conditions, its amino groups can be partially protonated resulting in repulsion between positively charged macrochains, thereby allowing diffusion of water molecules and subsequent solvation of macromolecules.

Water solubility of Chitosan and Chitosan-g-Octanal Schiff base derivatives is shown in Table 2. From the obtained results, it can be seen that the water solubility of CH-Oct0 significantly ($p < 0.05$) decreased after click reaction with Octanal and as the grafted Octanal percent increased from 38.25 G% (CH-Oct0.5) to 81.75 G% (CH-Oct5) where turned to be almost insoluble even at acidic pH medium. The decrease in CH-Oct0 solubility can be attributed to the formation of covalent imide bonds after click reaction of amine groups of CH-Oct0 with the aldehyde ones of Octanal. These findings in Table 2 acquired the developed CH-Oct0.5 and CH-Oct5 Schiff bases two desirable characteristics to be high-efficient oil sorbent, excellent hydrophobicity and low water uptake and solubility [4].

FTIR spectroscopy

The FT-IR spectra of the CH-Oct0, CH-Oct0.5 and CH-Oct5 were represented as shown in Fig. 1. The FT-IR chart illustrates the regular bands of CH-Oct0 function groups. A broadband around 3425 cm^{-1} corresponding to the stretching vibration of NH$_2$ and OH groups and O–H bending at 1394 cm^{-1} indicates the presence of hydroxyl groups [67]. The weak absorption peak is at 2895 cm^{-1} (C–H stretch) for methyl and methylene groups, and the characteristic peak of Chitosan at 1624 cm^{-1} assigned to the C=O stretching [68]. The band at 1070 cm^{-1} ascribed to the stretching of the C–O–C bridge [69]. Structural analysis of Octanal by FTIR spectrophotometer showed the identical spectrum with ν_{max}: 1720 (v C=O aldehyde), 2720 (v, C-H aldehyde) and 1380 cm^{-1} (ẟ-CH aldehyde) [70]. Chitosan-*g*-Octanal Schiff base shows significant FT-IR changes (Fig. 1; CH-Oct0.5 and CH-Oct5). The significant differences are:

(a) Firm absorption peaks at around 1566 cm−1 corresponding to the C=N stretching which formed between the aldehyde groups of Octanal and amine groups of CH-Oct0. It seems stronger in case of CH-Oct5 with 81.75 G% relative to CH-Oct0.5 with 38.25 G%.

(b) Absorption band at around 2937 cm−1 for Chitosan-g-Octanal Schiff base of -CH stretching which also seems stronger in case of CH-Oct5 relative to CH-Oct0.5, and.

Table 2 Solubility percent of Chitosan and its Schiff base derivative at different pH

pH	Solubility (W/V; %)		
	CH-Oct0	CH-Oct0.5	CH-Oct5
pH 3	99.88	99.78	1.78
pH 4	99.75	89.74	1.25
pH 5	96.37	71.82	0.19
pH 6	88.28	61.74	0*
pH 7	0*	0*	0*
pH 8	0*	0*	0*

0* means completely insoluble

(c)   Absorption band at around 1420 cm−1, which also seems stronger in case of CH-Oct5 relative to CH-Oct0.5, for the merger between –NHCO (Amide III) band at 1395 cm−1 of CH-Oct0 and –CH2 band at 1470 cm−1 and -CH band at 1380 cm−1 of the grafted Octanal [70].

TGA

Thermal gravimetric analysis (TGA) of CH-Oct0, CH-Oct0.5 and CH-Oct5 is presented in Fig. 2. The first weight loss that starts from ambient temperature to about 150 °C resulted from evaporation of moisture that attached from the atmosphere or during the reaction process. The increase of moisture content was attributed to the pseudo-hydrophilic character that associated with porous materials [65]. The subsequent degradation that recognized from 220 to 320 °C was a result of oxidative decomposition of the CH-Oct0. In this stage, first depression was produced from destruction of amine groups to form cross-linked fragments [70].

There is a significant difference in thermal stability between CH-Oct0, CH-Oct0.5 and CH-Oct5, where the temperature required to lose their half weights (T50%) is 343 °C, 385 °C and 325 °C as represented in Table 2. The stability of Schiff base derivatives is confirmed with previously published literature [64]. The third depuration that results from the decomposition which appears at high temperature may produce from the thermal degradation of a new cross-linked material formed by thermal crosslinking reactions occurring in the first stage of the degradation process [71].

Interestingly, CH-Oct0.5 and CH-Oct5 have overall higher stability than CH-Oct0 at 600◦C where 36.46% and 25.86% of CH-Oct5 and CH-Oct0.5 residues left, but in case of CH-Oct0, only 8.43% was remained (Table 3) [72].This finding proves the changes caused by grafting of the hydrophobic Octanal chains onto amine groups of Chitosan.
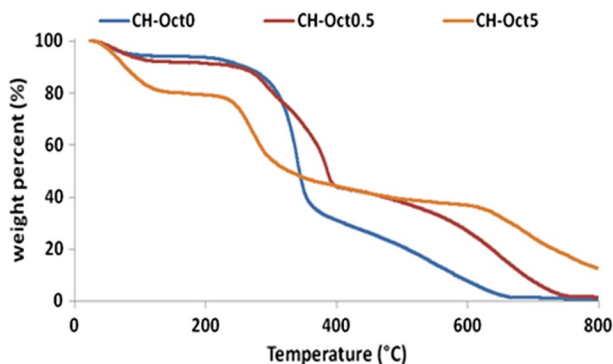

Fig. 2 TGA of Chitosan and Chitosan-g-Octanal Schiff base derivatives

Table 3 Thermal gravimetric peaks of Chitosan and Chitosan-g-Octanal Schiff bases

| Sample	Loss (W%) at 150 °C	T25% (°C)	T50% (°C)	Loss (W%) at 600 °C	Residual (W%) at 600 °C
CH-Oct0	6.02	319.34	342.81	91.57	8.43
CH-Oct0.5	8.24	323.48	385.49	74.14	25.86
CH-Oct5	19.86	246.61	325.74	63.54	36.46

SEM

A scanning electron microscope studied the surface morphological analysis of CH-Oct0, CH-Oct0.5 and CH-Oct5 matrices with different grafting percentages (Fig. 3). The SEM graphs show changes in the surface morphology as the CH-Oct0.5 and CH-Oct5 Schiff base formation [73]. The Chitosan-*g*-Octanal Schiff base with 38.25 G% grafting percentage, (b) CH-Oct0.5, shows a mix of microparticles structures with different sizes and foils structure. Different exciting changes of Chitosan-*g*-Octanal Schiff base of 81.75 G% structure have been noticed and more surface roughness obtained covered with homogenous particles structure ((c) CH-Oct 5). Different shapes may attribute to the acquired variant of amphiphilic character resulting from the hydrophilic-hydrophobic balance of the CH-Oct0 and the newly formed CH-Oct0.5 and CH-Oct5 Schiff bases. Moreover, the water content plays a fetal role in the arrangement of the polymers chains and, accordingly, the formed polymer structures.

Kinetics, isotherms and thermodynamics of oil spills removal

Effect of the adsorption time and kinetics

The effect of variation the adsorption time from 10 to 180 min on oil adsorption percentage of heavy crude oil for the CH-Oct0 and CH-Oct5 Schiff bases adsorbents is studied in Fig. 4A. The conduct experiment was carried out under dynamic condition by the addition of 0.1 g of sorbent material over the oil/artificial sea water surface using heavy crude oil.

On the other hand, Fig. 4A reveals that the oil adsorption percentage by CH-Oct5 Schiff base was doubled of the CH-Oct0 at equilibrium. This behavior is expected, due to the hydrophobic nature of the CH-Oct5 Schiff base sorbent material which enable them to attach oil molecules easily on the adsorbent surface and inside their porous structures. Therefore, the number of attached molecules increased by increase the contact time between oil and the CH-Oct5 Schiff base adsorbent improving its adsorption capacity. However, after a certain time, the sorbent material became saturated and its affinity towards oil molecules decreased [74]. Moreover, it was observed that the highest heavy crude oil adsorption percentage % values were recorded 92% for CH-Oct5 Schiff base at equilibrium [75].

Chitosan (a)

Chitosan-g-Octanal 38.25 G% (b)

Chitosan-g-Octanal 81.75 G% (g).
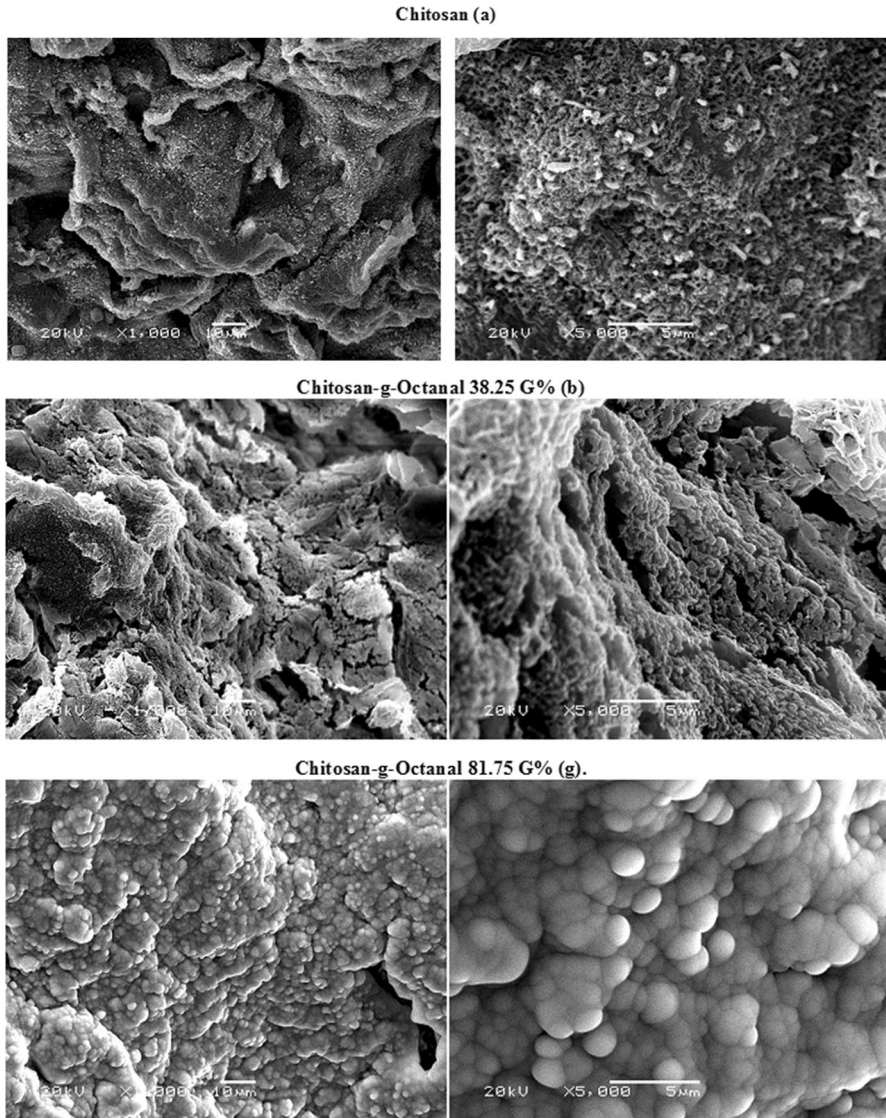
Fig. 3 SEM photographs, 1000× and 5000x, of **a** CH-Oct0 **b** CH-Oct0.5 and **c** CH-Oct5

The knowledge of adsorption kinetics is important information for designing batch adsorption systems. To examine the adsorption kinetics of CH-Oct0 and CH-Oct5 Schiff bases for heavy crude oil, the pseudo-first-order and pseudo-second-order kinetic models and intraparticle diffusion model were examined [24, 67, 76].

(1) *Pseudo-first-order kinetic model*

$$\log\left(q_e - q_t\right) = \log q_e - \frac{k_1}{2.303}t \tag{5}$$

(2) *Pseudo-second-order kinetic model*

$$\frac{t}{q_t} = \frac{1}{k_2 q_e^2} + \frac{t}{q_e} \tag{6}$$

where q_e is the amount of adsorption at equilibrium, g/g; q_t is the amount of adsorption at time t, g/g; k_1 is the first-order rate constant, min^{-1}; k_2 is the second-order rate constants, min^{-1}.

Constants of pseudo-first-order and pseudo-second-order were determined experimentally by plotting of log $(q_e - q_t)$ versus t for pseudo-first-order (Fig. 4B) and by plotting a t/q_t against t (Fig. 4C). From the figures, it is clear that the pseudo-first- and second-order reaction rate models adequately describe the kinetics of heavy crude oil sorption with a high correlation coefficient: consequently, it was further used to describe all the kinetics of heavy crude oil sorption by CH-Oct0 and CH-Oct5 Schiff bases (Tables 4 and 5).

The conformity between experimental data and the model predicted values was expressed by correlation coefficient (R^2). Comparing Fig. 4B with Fig. 4C, it is found that the pseudo-second-order equation fitted the experimental data better than the pseudo-first-order equation for its higher R^2 (all R^2 values are closed to 1) [76]. The amount of adsorption equilibrium q_e, the rate constants of the equation, k_1 and k_2, the calculated amount of adsorption equilibrium, $q_{e(cal.)}$, and the coefficient of determination, R^2, for heavy oil are shown in Tables 3 and 4.

It can be seen in Tables 4 and 5 that, with an increase in initial amount of oil, the initial adsorption rate (h_0) increases while the rate constant of adsorption (k_2) almost decreases. A similar observation was also reported by the earlier researchers [77, 78]. Meanwhile, the calculated amount of adsorption equilibrium ($q_{e(cal.)}$) from the pseudo-second-order equation is close to the actual amount of adsorption equilibrium ($q_{e(exp.)}$).

It can be seen in Table 6 that oil adsorption rate constant k_2 in case of CH-Oct0 greater than CH-Oct5 Schiff bases which indicate faster rate diffusion of heavy oils in case of adsorption by CH-Oct0, but adsorption capacity (q_e) of CH-Oct5 Schiff bases is higher than of CH-Oct0 in case of heavy crude oil [76].

(3) *Intra-particle diffusion model:*

$$q_t = K_p t^{0.5} + C \tag{7}$$

where kp is the intraparticle diffusion constant (g/g $min^{1/2}$). If the intra-particle diffusion is involved in the adsorption process, then a plot of the amount of oil adsorbed per unit mass of adsorbent (q_t) against square root of time ($t^{1/2}$) gave a straight-line and the particle diffusion would be the controlling step if this line passed through the origin [71, 79].

Figure 4D demonstrates the plot of oil sorption capacity q_t (g/g), versus $t^{1/2}$ for heavy crude oil adsorption. The deviation of straight lines from the origin indicates that intra-particle transport is not the rate-limiting step. As seen from this figure, the intra-particle diffusion rate equation fits well to the initial stages of the adsorption process for all the tested CH-Oct0 and CH-Oct5 Schiff bases.

From Table 4 it is obvious that values of $\mathbf{K_p}$ for CH-Oct0 increase from 0.292 to 0.806 g/g.min$^{0.5}$, and values of $\mathbf{K_p}$ for CH-Oct5 Schiff bases (Table 5) increase from 0.468 to 2.12 g/g.min$^{0.5}$ when the initial amount of heavy crude oil was increased from 0.5 to 2.5 g. This is because increasing initial amount of oil facilitates oil diffusion inside the adsorbent particles [80].

Table 6 shows the calculated values of $\mathbf{K_p}$ for CH-Oct5 Schiff base are higher than $\mathbf{K_p}$ for CH-Oct0 due to oil diffusion inside the adsorbent particle in case of CH-Oct5 Schiff base is higher than in case of CH-Oct0.

Effect of the oil amount and adsorption isotherm

To study the effect of the amount of oil on the adsorption percentage (%) of oil on CH-Oct0 and CH-Oct5 Schiff base, different oil amounts were experimented (Fig. 5A). In brief, 0.1 g of the sorbent material was added to the oil/artificial sea water system using different weights of heavy crude oil (0.5, 1,1.5, 2 and 2.5 g) at constant artificial seawater (20 ml) [6]**.** The progressive decrease of oil adsorption percentage was observed with the increase in the amount of heavy crude oil from 0.5 to 2.5 g [75].

Generally, increasing the oil amount provides an important driving force to overcome all resistances of the oil between the aqueous and solid phases, thus increasing the uptake. In addition, increasing the initial oil concentration increases the number of collisions between oil and the adsorbent, which enhances the sorption capacity [65, 81]. On the other hand, increasing weight of the initial crude oil is reflected reversely on the oil adsorption percentage because the definition of the oil adsorption percentage of the sorbent is as the ratio of the weight of adsorbed oil to the initial weight of oil. Accordingly, the oil adsorption percentage takes negative trend with the initial amount of oil [65, 75].

The adsorption isotherm indicates how the adsorbate molecules distribute between the liquid phase and the solid phase at equilibrium. The analysis of the isotherm data by fitting them to different isotherm models is an important step to find the suitable model that can be used for design purpose..In this research, adsorption isotherm study was carried out on two well-known isotherms, i.e., Langmuir and Freundlich [65, 82].
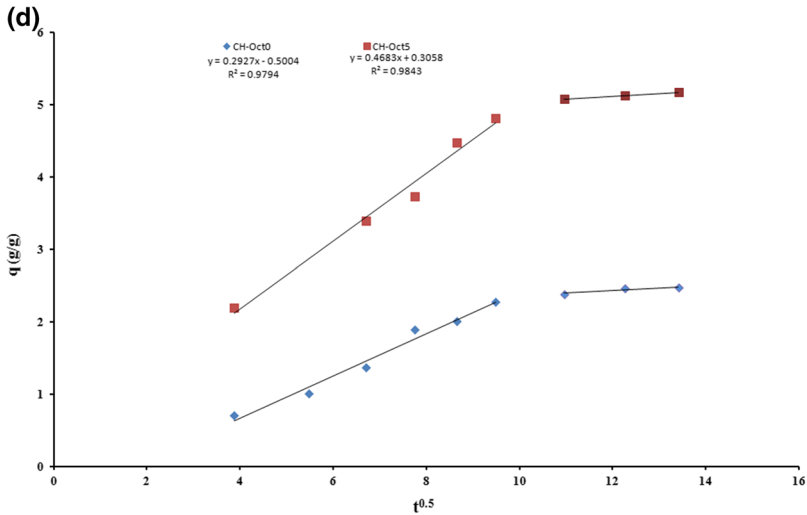
(d)
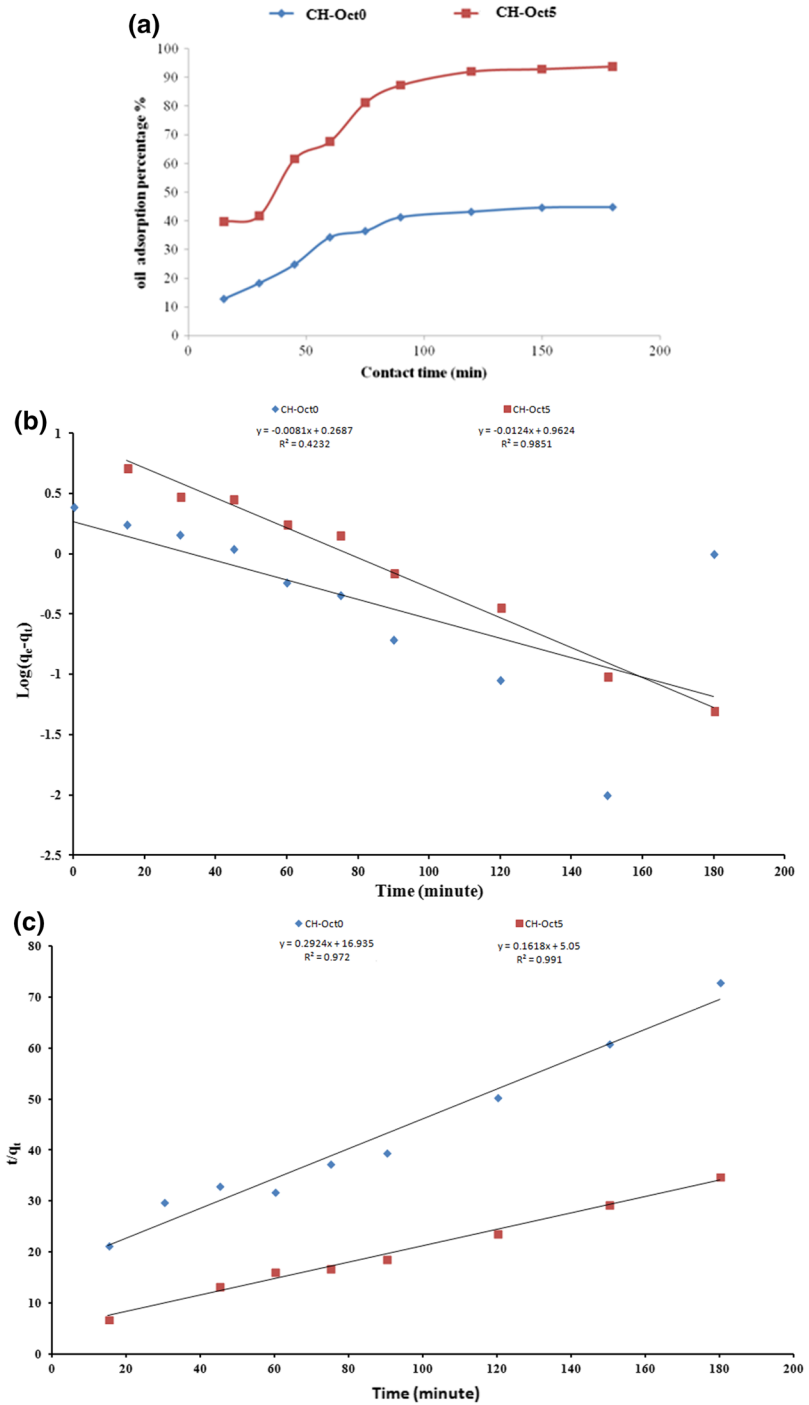
Fig. 4 (continued)

Langmuir and Freundlich models The Langmuir model is obtained below the ideal assumption of a totally homogenous adsorption surface and represented as follows [65, 77, 79]:

$$C_e/q_e = \frac{1}{q_{max}b} + \frac{C_e}{q_{max}} \tag{8}$$

where q_e is the oil uptake at equilibrium (g/g); q_{max} is the maximum Langmuir uptake (g/g); C_e is the final oil concentration at equilibrium (g/l); b is the Langmuir affinity constant (L/g).

Figure 5B shows the Langmuir plots heavy crude oil at different temperatures by (a) CH-Oct0 and (b) CH-Oct5 Schiff base. The Langmuir isotherm constants q_m and b were calculated from the particular slope and intercept of the linear plot of C_e/q_e vs. C_e, and the values are presented in Table 7. It can be seen that the maximum adsorption capacity (q_m) and b constants increased with increasing temperature, which indicates the endothermic nature of the adsorption process [24, 83].

The important features of the Langmuir isotherm can be expressed in terms of a dimensionless constant separation factor (R_L), which is defined as [67]:

$$R_L = \frac{1}{1 + bC_o} \tag{9}$$

where b is the Langmuir constant and C_0 is the initial oil concentration (g L^{-1}), and the value of R_L indicates the type of isotherm to be either unfavorable ($R_L > 1$), linear ($R_L = 1$), favorable ($0 < R_L < 1$) or irreversible ($R_L = 0$) [79]. The calculated R_L values at different amounts of heavy crude oil for CH-Oct0 and CH-Oct5 Schiff bases are shown in Fig. 5C. It can be seen that R_L value drops into the range 0–1 in all experimental systems, which confirms the favorable uptake of the heavy oil

Table 4 Kinetic parameters for heavy crude oil adsorption using Chitosan different initial amounts of oil

Adsorption condition & adsorption capacity		Kinetic models									
Amount of oil (g)	$q_{e(exp)}$ (g g^{-1})	Pseudo-first- order			Pseudo-second- order				Intra-particle diffusion		
		$q_{e(cal)}$ (g g^{-1})	K_1 (gg^{-1} min^{-1})	R^2	$q_{e(cal)}$ (g g^{-1})	K_2 (gg^{-1} min^{-1})	h_0 (g g^{-1} min^{-1})	R^2	K_P (g g^{-1} min$^{-1/2}$)	C (g g^{-1})	R^2
0.5	2.474	1.85	0.0184	0.423	3.05	0.0053	0.0489	0.959	0.292	−0.5	0.979
1	5.768	4.93	0.0161	0.646	7.35	0.0019	0.103	0.963	0.648	−1.117	0.957
1.5	6.75	6.62	0.0161	0.772	10.87	0.0007	0.087	0.958	0.747	−1.7	0.99
2	8.449	8.51	0.0138	0.88	15.625	0.00087	0.1125	0.967	0.708	−0.63	0.949
2.5	9.915	10.42	0.0138	0.923	19.23	0.00033	0.1219	0.973	0.806	−0.772	0.946

Table 5 Kinetic parameters for heavy crude oil adsorption using Chitosan-g-Octanal Schiff base at different initial amounts of oil

Adsorption condition & adsorption capacity		Kinetic models									
Amount of oil (g)	$q_{e(exp)}$ (g g^{-1})	Pseudo-first-order			Pseudo-second-order				Intra-particle diffusion		
		$q_{e(cal)}$ (g g^{-1})	K_1 (gg^{-1} min^{-1})	R^2	$q_{e(cal)}$ (g g^{-1})	k_2 (gg^{-1} min^{-1})	h_0 (g g^{-1} min^{-1})	R^2	K_P (g g^{-1} min$^{-1/2}$)	C (g g^{-1})	R^2
0.5	5.174	9.16	0.0276	0.985	6.21	0.0051	0.1980	0.991	0.468	−0.305	0.984
1	12.369	22.59	0.0276	0.976	14.93	0.002	0.451	0.989	1.199	−0.131	0.95
1.5	15.243	50.47	0.0368	0.898	19.61	0.0011	0.436	0.975	1.444	−0.326	0.967
2	19.54	33.49	0.0253	0.959	25	0.00088	0.5470	0.985	1.657	−1.414	0.921
2.5	22.21	26.85	0.0207	0.985	30.303	0.00062	0.5695	0.982	2.12	−0.977	0.969

Table 6 Kinetic parameters for heavy crude oil adsorption with Chitosan and Chitosan-g-Octanal Schiff base at fixed initial oil concentration

Adsorbent	Adsorption capacity $q_{e(exp)}$ ($g\,g^{-1}$)	Pseudo-first-order			Pseudo-second-order				Intra-particle diffusion		
		$q_{e(cal)}$ ($g\,g^{-1}$)	K_1 ($gg^{-1}\,min^{-1}$)	R^2	$q_{e(cal)}$ ($g\,g^{-1}$)	k_2 ($gg^{-1}\,min^{-1}$)	h_0 ($g\,g^{-1}\,min^{-1}$)	R^2	K_P ($g\,g^{-1}\,min^{-1/2}$)	C ($g\,g^{-1}$)	R^2
Chitosan	2.474	1.85	0.0184	0.423	3.42	0.0063	0.059	0.972	0.292	− 0.5	0.979
Chitosan-g-Octanal Schiff base	5.174	9.16	0.0276	0.985	6.21	0.0051	0.1980	0.991	0.468	− 0.305	0.984

process. Lower R_L values at higher amount of oil showed that adsorption was more favorable at higher amount of oil.

The empirical Freundlich isotherm, based on sorption on heterogeneous surface, can be derived assuming a logarithmic decrease in the enthalpy of sorption with the increase in the fraction of occupied sites and is given by [65, 76]:

$$q_e = k_f C_e^{1/n} \tag{10}$$

where K_F and $1/n$ are the Freundlich constants characteristics of the system, indicating the sorption capacity and sorption intensity.

Respectively, (Eq. 8) can be linearized in logarithmic form (Eq. 10) and the Freundlich constants can be determined from their intercept and slope.

$$\log q_e = \log K_F + \frac{1}{n} \log C_e \tag{11}$$

Figure 5D gives an idea about the Freundlich plots of heavy crude oil at different temperatures by CH-Oct0 and CH-Oct5 Schiff bases, and at room temperature by CH-Oct0 and CH-Oct5 Schiff bases [79]. The Freundlich isotherm constants K_F and $1/n$ in case of heavy oil were calculated from the particular slope and intercept of the linear plot of $\log q_e$ vs. $\log C_e$, and the values are presented in Table 7. Here, the intensity parameter $1/n$ indicates the deviation of the adsorption isotherm from linearity. $1/n < 1$ shows that the adsorption is favorable, new adsorption sites are available and the adsorption capacity increases. $1/n > 1$ indicates that the adsorption bonds are weak, adsorption capacities decrease and un-favorable.

From Table 7 the values of $1/n$ less than 1 represent a favorable adsorption [59]. The k_F values of CH-Oct0 and CH-Oct5 Schiff bases were found to increase with the increase in temperature. This confirms the endothermic nature of sorption [79].

From the correlation coefficient R^2 values indicate a good mathematical fit that adsorption process of heavy crude oil more fitted to Langmuir model. So, adsorption of heavy crude oil by CH-Oct0 and CH-Oct5 Schiff bases adsorbents described to occur on a totally homogenous and monolayer adsorption surface [24].

Adsorption thermodynamics

The thermodynamic parameters, such as change in Gibbs free energy (ΔG^0), change in enthalpy (ΔH^0) and change in entropy (ΔS^0) of light and heavy oil adsorbed by CH-Oct0 and CH-Oct5 Schiff bases, are calculated by Eqs. (12–14) [65, 79]:

The Gibbs free energy change of the adsorption process is related to the equilibrium constant by the equation:
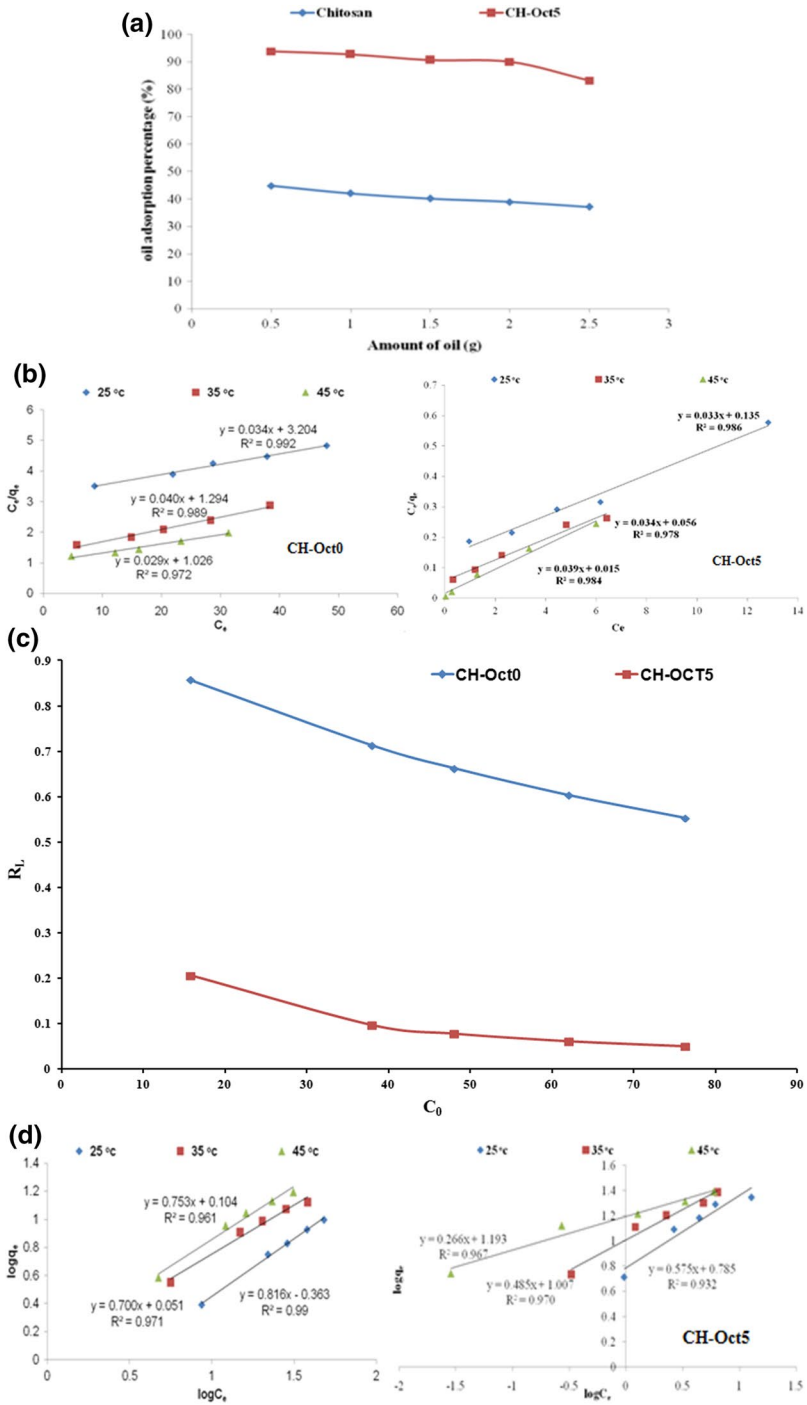
Table 7 Isotherm parameters for heavy crude oil adsorption onto Chitosan and Chitosan-g-Octanal Schiff base at different temperatures

Langmuir isotherm						Freundlich isotherm					
Chitosan			Chitosan-g-Octanal Schiff base			Chitosan			Chitosan-g-Octanal Schiff base		
b	q_{max}	R^2	b	q_{max}	R^2	k_F	1/n	R^2	k_F	1/n	R^2
At 25°c											
0.011	29.4	0.992	0.244	30.3	0.986	0.43	0.81	0.99	6.095	0.575	0.932
Chitosan			Chitosan-g-Octanal Schiff base			Chitosan			Chitosan-g-Octanal Schiff base		
b	q_{max}	R^2	b	q_{max}	R^2	k_F	1/n	R^2	k_F	1/n	R^2
At 35°c											
0.03	25	0.989	0.61	29.4	0.978	1.125	0.69	0.971	10.16	0.49	0.97
At 45°c											
0.028	34.48	0.972	2.6	25.64	0.984	1.27	0.75	0.961	11.024	0.266	0.967

$$\Delta G° = -RT \ln b \tag{12}$$

where $\Delta G°$ is the standard free energy change (KJ mol^{-1}), T the absolute temperature (K) and R (8.3145 J/(mol·K)) is the ideal gas constant, b (mg g^{-1}) an equilibrium constant obtained Langmuir constant.

According to thermodynamics, the Gibbs free energy change is also related to the entropy change and heat of adsorption at constant temperature by the following equation:

$$\Delta G° = \Delta H^{\mathbf{o}} - T\Delta S^{o} \tag{13}$$

$$\text{Ln } b = (\Delta S/R) - (\Delta H/RT) \tag{14}$$

where $\Delta H°$ is enthalpy change (KJ mol -1), $\Delta S°$ entropy change (KJ mol^{-1} K^{-1}), $\Delta H°$ and $\Delta S°$ can be calculated from the plot of (ln b) versus (1/T).

The values of $\Delta S°$ and $\Delta H°$ are calculated from the slopes and intercepts of the linear plots of lnb versus 1/T (Fig. 6), $\Delta G°$ is obtained using (Eq. 12). The thermodynamic parameters of heavy oil adsorbed by CH-Oct0 and CH-Oct5 Schiff bases adsorbents are listed in Table 8. The positive values of $\Delta H°$ suggest that the interaction of heavy oil adsorbed by CH-Oct0 and CH-Oct5 Schiff bases adsorbents is endothermic, which is supported by the increase adsorption of heavy crude oil with a rise in temperature [69]. The negative value of $\Delta G°$ indicates the spontaneous nature of the adsorption. $\Delta G°$ value is decreasing with increasing temperature, which suggests that higher temperature makes the adsorption easier.

The positive entropy $\Delta S°$ of CH-Oct0 and CH-Oct5 Schiff bases indicates that process was caused by the decrease in degree of freedom of the adsorbed species and this positive value of heavy crude oil suggested that the randomness
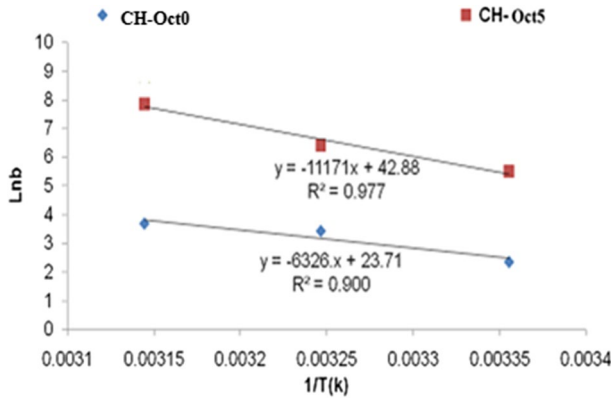
Fig. 6 Chitosan and Chitosan-g-Octanal Schiff base Van t' Hoff graph of heavy crude oil adsorption

Table 8 Thermodynamics parameter for the adsorption of heavy oil onto Chitosan and Chitosan-g-Octanal Schiff base adsorbents

T (°C)	Ln b	Δ G (KJ/mol)	Δ S (kJ/mol K)	Δ H (KJ/mol)	R^2
Chitosan					
25	2.36	− 7.99	0.197	52.59	0.900
35	3.43	− 8.79			
45	3.69	− 9.61			
Chitosan-g-Octanal Schiff base					
25	5.49	− 12.99	0.357	92.88	0.977
35	6.41	− 15.72			
45	5.49	− 12.99			

increased at the solid–liquid interface during the adsorption of heavy oil on CH-Oct0 and CH-Oct5 Schiff bases [76].

Conclusion

The present work investigates the kinetic, isothermal and thermodynamic of the oil spills removal process conducted by adsorption onto Chitosan and novel amphiphilic Chitosan-g-Octanal Schiff base adsorbents, developed by click chemistry. The developed novel Chitosan Schiff base compounds were characterized under advanced analytical tools such as Fourier transform infrared spectroscopy (FTIR), thermal analysis (TGA) and SEM analysis.

The developed Chitosan-g-Octanal Schiff base adsorbent turns to be hydrophobic where no water uptake was detected compared with Chitosan adsorbent; 1.45 g/g. The ion exchange capacity confirmed that behavior where decreased from 9.95 meq/g of Chitosan adsorbent to 1.47 meq/g of Chitosan-g-Octanal Schiff base

adsorbent. The obtained results revealed that there was a major increase in the oil adsorption capacity of Chitosan-g-Octanal Schiff base adsorbent compared to the Chitosan due to increasing its hydrophobic characters after Schiff base formation, where the maximum oil adsorption percentage (%) recorded using heavy crude oil was 96.41% for Chitosan-g-Octanal Schiff base adsorbent compared to 64.99% for Chitosan counterpart. In addition, high rate of adsorption was observed where 40% of oil adsorbed within 15 min only using the Chitosan-g-Octanal Schiff base adsorbent compared to 90 min for native Chitosan one. The adsorption process followed the pseudo-second order model and the equilibrium data were sufficiently fitted with the Langmuir model with a maximum adsorption capacity 30.30 g/g at 25 °C. Thermodynamic parameters computed from Van't Hoff plot confirmed the process to be endothermic, favorable and spontaneous.

The results nominate the developed hydrophobic Chitosan-g-Octanal Schiff base adsorbent as a potential adsorbent for petroleum oil spills removal.

References

1. Ali I, Jain CK (1998) Groundwater contamination and health hazards by some of the most commonly used pesticides. Curr Sci 75:1011–1014
2. Ali I, Gupta VK, Aboul-Enein HY (2005) Metal ion speciation and capillary electrophoresis: application in the new millennium. Electrophoresis 26:3988–4002
3. Basheer A (2018) Chemical chiral pollution: impact on the society and science and need of the regulations in the 21st century. Chirality 30:402–406
4. Basheer A (2018) New generation nano-adsorbents for the removal of emerging contaminants in water. J Mol Liq 261:583–593
5. Basheer A, Ali I (2018) Stereoselective uptake and degradation of (±) o, p DDD pesticide stereomers in water sediment system. Chirality 30:1088–1095
6. Ali I, Aboul-Enein HY (2002) Speciation of metal ions by capillary electrophoresis. Crit Rev Anal Chem 32:337–350
7. Ali I, Alharbi OML, Alothman ZA, Alwarthan A (2018) Facile and eco-friendly synthesis of functionalized iron nanoparticles for cyanazine removal in water. Colloids Surf B 171:606–613
8. Burakova EA, Dyachkova TP, Rukhov AV, Tugolukov EN, Galunin EV, Tkachev AG, Basheer A, Ali I (2018) Novel and economic method of carbon nanotubes synthesis on a nickel magnesium oxide catalyst using microwave radiation. J Mol Liq 253:340–346

9. Ali I, Alharbi OML, Alothman ZA, Badjah AY (2018) Kinetics, thermodynamics, and modeling of amido black dye photodegradation in water using Co/TiO2 nanoparticles. Photochem Photobiol 94:935–941

10. Ali I, Alharbi OML, ALOthman ZA, Alwarthan A, Al-Mohaimeed AM (2019) Preparation of a carboxymethylcellulose-iron composite for uptake of atorvastatin in water. Int J Biol Macromol 132:244–253

11. Ali I, Alharbi OML, Alothman ZA, Al-Mohaimeed AM, Alwarthan A (2019) Modeling of fenuron pesticide adsorption on CNTs for mechanistic insight and removal in water. Environ Res 170:389–397

12. Ali I, Afshinb S, Poureshgh Y, Azari A, Rashtbari Y, Feizizadeh A, Hamzezadeh A, Fazlzadeh M (2020) Green preparation of activated carbon from pomegranate peel coated with zero-valent iron nanoparticles (nZVI) and isotherm and kinetic studies of amoxicillin removal in water. Environ Sci Pollut Res 27:36732–36743

13. Ali I, Babkin AV, Burakova IV, Burakov AE, Neskoromnaya EA, Tkachev AG, Panglisch S, AlMasoud N, Alomar TS (2021) Fast removal of samarium ions in water on highly efficient nanocomposite based graphene oxidemodified with polyhydroquinone: Isotherms, kinetics, thermodynamics and desorption. J Mol Liq 329:115584

14. Ali I, Kon'kova T, Kasianov V, Rysev A, Panglisch S, Mbianda XY, Habila MA, AlMasoud N (2021) Preparation and characterization of nano-structured modified montmorillonite for dioxidine antibacterial drug removal in water. J Mol Liq 331:115770

15. Ali I, Alharbi OML, Tkachev A, Galunin E, Burakov A, Grachev VA (2018) Water treatment by new-generation graphene materials: hope for bright future. Environ Sci Pollut Res 25:7315–7329

16. Ali I, Burakov AE, Melezhik AV, Babkin AV, Burakova IV, MsEA N, Galunin EV, Tkachev AG, Kuznetsov DV (2019) Removal of copper(II) and zinc(II) ions in water on a newly synthesized polyhydroquinone/graphene nanocomposite material: kinetics, thermodynamics and mechanism. Chem Select 4:12708–12718

17. Hussein M, Amer AA, Sawsan II (2008) Oil spill sorption using carbonized pith bagasse: trial for practical application. Int J Environ Sci Technol 5:223–242

18. Nwankwere ET, Gimba CE, Kagbu JA, Nale BK (2010) Sorption studies of crude oil on acetylated rice husks. Adv Appl Sci Res 2:142–145

19. Nwadiogbu JO, Ajiwe VIE, Okoye PAC (2016) Removal of crude oil from aqueous medium by sorption on hydrophobic corncobs: equilibrium and kinetic studies. J Taibah Univ Sci 10:56–63

20. Adebajo MO, Frost RL, Kloprogge JT, Carmody O, Kokot S (2003) Porous materials for oil spill cleanup: a review of synthesis and absorbing properties. J Porous Mater 10:159–170

21. Srinivasan A, Viraraghavan T (2010) Oil removal from water using biomaterials. Biores Technol 101:6594–6600

22. Moura FCC, Lago RM (2009) Catalytic growth of carbon nanotubes and nanofibers on vermiculite to produce floatable hydrophobic '"nanosponges"' for oil spill remediation. Appl Catal B 90:436–440

23. Lin JY, Shang YW, Ding B, Yang JM, Yu JY, Al-Deyab SS (2012) Nanoporous polystyrene fibers for oil spill cleanup. Mar Pollut Bull 64:347–352

24. Jintao W, Yian Z, Aiqin W (2013) Coated kapok fiber for removal of spilled oil. Mar Pollut Bull 69:91–96

25. Francis S, Matthew JK, Howard WT (2000) Application of chitosan-based polysaccharide biomaterials in cartilage tissue engineering: a review. Biomaterials 21:2589–2598

26. Hirano S, Tsuchida H, Nagao N (1989) *N*-acetylation in chitosan and the rate of its enzymic hydrolysis. Biomaterials 10:574–576

27. Kofuji K, Qian CJ, Nishimura M, Sugiyama I, Murata Y, Kawa-shima S (2005) Relationship between physicochemical characteristics and functional properties of chitosan. Eur Polym J 41:2784–2791

28. Mohy Eldin MS, Ammar YA, Tamer TM, Omer AM, Ali AA (2016) Development of oleophilic adsorbent based on chitosan–poly (butyl acrylate) graft copolymer for petroleum oil spill removal. Int J Adv Res 4:2095–2111

29. Baxter A, Dillon M, Anthony KD, George T, Roberts AF (1992) Improved method for i.r. determination of the degree of *N*-acetylation of chitosan. Int J Bio Macromol 14:166–169

30. Nwe N, Furuike T, Tamura H (2009) The mechanical and biological properties of chitosan scaffolds for tissue regeneration templates are significantly enhanced by chitosan from Gongronella butleri. Materials 2:374–398

31. Rinaudo M (2006) Chitin and chitosan: properties and applications. Prog Polym Sci 31:603–632

32. Aziz NAA, Abu Bakar A, Hassan A, Azmi N (2014) Synthesis of chitosan-grafted-poly(methyl methacrylate) with fenton's reagent (Fe^{2+}-H_2O_2) as a redox initiator. Malays J Anal Sci 18:415–422

33. Tavakol M, Vasheghani-Farahani E, Hashemi-Najafabadi S (2013) The effect of polymer and $CaCl_2$ concentrationson the sulfasalazine release from alginate-N. O-carboxymethyl Chitosan Beads Prog Biomater 2:10

34. Madhusudhan A, Reddy GB, Venkatesham M, Veerabhadram G, Kumar DA, Natarajan S, Yang M-Y, Hu A, Singh SS (2014) Efficient pH dependent drug delivery to target cancer cells by gold nanoparticles capped with carboxymethyl chitosan. Int J Mol Sci 15:8216–8234

35. Sokker HH, El-Sawy NM, Hassan MA, El-Anadouli BE (2011) Adsorption of crude oil from aqueous solution by hydrogel of chitosan based polyacrylamide prepared by radiation induced graft polymerization. J Hazard Mater 190:359–365

36. Mohy Eldin MS, Soliman EA, Hashem AI, Tamer TM (2012) Antimicrobial activity of novel aminated chitosan derivatives for biomedical applications. Adv Polym Technol 31:414–428

37. Muzzarelli RAA, Jeunieux C, Gooday GW (1985) Chitin in nature and technology. Plenum, New York

38. Moore GK, Roberts GAF (1981) Reactions of chitosan: preparation and reactivity of Schiff's base derivatives of chitosan. Int J Biol Macromol 3:337–341

39. Sashikala S, Syed Shafi S (2014) Synthesis and characterization of chitosan Schiff base derivatives. Pharm Lett 6:90–97

40. Francisco C, Luiz CGV, Técia VC, Ronaldo FDN (2014) Removal of petroleum spill in water by chitin and chitosan. Orbital Electron J Chem 6:70–74

41. Gupta RK, Dunderdale GJ, England MW, Hozumi A (2017) Oil/water separation techniques: a review of recent progresses and future directions. J Mater Chem A 5:16025–16058

42. Wei QF, Mather RR, Fotheringham AF, Yang RD (2003) Evaluation of nonwoven polypropylene oil sorbents in marine oil-spill recovery. Mar Pollut Bull 46:780–783

43. Doshi B, Sillanpää M, Kalliola S (2018) A review of bio-based materials for oil spill treatment. Water Res 135:262–277

44. Venkataraman P, Tang J, Frenkel E, McPherson GL, He J, Raghavan SR, Kolesnichenko V, Bose A, John VT (2013) Attachment of a hydrophobically modified biopolymer at the oil-water interface in the treatment of oil spills. ACS Appl Mater Interfaces 5:3572–3580

45. Sidik SM, Jalil AA, Triwahyono S, Adam SH, Satar MAH, Hameed BH (2012) Modified oil palm leaves adsorbent with enhanced hydrophobicity for crude oil removal. Chem Eng J 203:9–18

46. Keshawy M, El-Moghny TA, Abdul-Raheim A-RM, Kabel K, El-Hamouly SH (2013) Synthesis and characterization of oil sorbent based on hydroxypropyl cellulose acrylate. Egypt J Pet 22:539–548

47. Sokker HH, El-Sawy NM, Hassan MA, El-Anadouli BE (2011) Adsorption of crude oil from aqueous solution by hydrogel of chitosan based polyacrylamide prepared by radiation induced graft polymerization. J Hazard Mater 190:359–365

48. Chauhan GS, Singh B, Kumar S, Chinkara A (2005) Synthesis and characterization of reactive copolymers of poly (butyl acrylate) and cellulose. Polym Polym Compos 13:467–477

49. Mohy Eldin MS, Ammar YA, Tamer TM, Omer AM, Ali AA (2017) Development of low-cost chitosan derivatives based on marine waste sources as oil adsorptive materials: I. preparation and characterization. Desal Water Treat 72:41–51

50. Liang XX, Omer AM, Hu Z, Wang Y, Yu D, Ouyang X (2018) Efficient adsorption of diclofenac sodium from aqueous solutions using magnetic amine-functionalized chitosan. Chemosphere 217:270–278

51. Eskhan A, Banat F, Abu Haija M, Al-Asheh S (2019) Synthesis of mesoporous/macroporous microparticles using three dimensional assembly of chitosan-functionalized halloysite nanotubes and their performance in the adsorptive removal of oil droplets from water. Langmuir 35:2343–2357

52. Mourya VK, Inamdar NN (2008) Chitosan-modifications and applications: opportunities galore. React Funct Polym 68:1013–1051

53. Mohy Eldin MS, Ammar YA, Tamer TM, Omer AM, Ali AA (2016) Development of oleophilic adsorbent based on chitosan- poly (butyl acrylate) graft copolymer for petroleum oil spill removal. Int J Adv Res 4:2095–2111

54. Benner SW, John VT, Hall CK (2015) Simulation study of hydrophobically modified chitosan as an oil dispersant additive. J Phys Chem B 119:6979–6990

55. Tamer MT, Katarína V, Mohamed AH, Ahmed MO, Muhammad E-S, Mohamed SM-E, Ladislav Š (2018) Chitosan/hyaluronan/edaravone membranes for anti-inflammatory wound dressing: in vitro and in vivo evaluation studies. Mater Sci Eng C 90:227–235

56. Jenkins DW, Samuel MH (2001) Review of vinyl graft copolymerization featuring recent advances toward controlled radical-based reactions and illustrated with chitin/chitosan, Trunk Polymers. Chem Rev 101:3245–3273

57. Nithya R, Sudha PN (2014) Grafting of N-butyl acrylate on to chitosan by ceric Ion initiation and its antimicrobial activity. Der Pharm Lett 6:58–64

58. Mohamed AH, Ahmed MO, Eman A, Walid MAB, Tamer MT (2018) Preparation, physicochemical characterization and antimicrobial activities of novel two phenolic chitosan Schiff base derivatives. Sci Rep 8:1–14

59. Islam MdM, Md MS, Rahman MM, Molla MdAI, Shaikhc AA, Roy SK (2011) Preparation of chitosan from shrimp shell and investigation of its properties. Int J Basic Appl Sci 11:77–80

60. Rigby G (1936) Substantially undegraded deacetylated chitin and processes for producing the same. Patent USA 2(040):879

61. Signini R, Campana Filho SPC (1999) On the preparation and characterization of chitosan hydrochloride. Polym Bull 42:159–166

62. Tamer TM, Hassan MA, Omer AM, Baset WMA, Hassan ME, El-Shafeey MEA, Mohy Eldin MS (2016) Synthesis, characterization and antimicrobial evaluation of two aromatic chitosan Schiff base derivatives. Process Biochem 51:1721–1730

63. Mohy Eldin MS, Omer AM, Hashem AI, Tamer TM (2015) Preparation, characterization and antimicrobial evaluation of novel cinnamyl chitosan Schiff base. Int J Adv Res 3:741–755

64. Kenawy ER, Abdel-Hay FI, Mohy Eldin MS, Tamer TM, Ibrahim EMAE (2015) Novel aminated chitosan-aromatic aldehydes schiff bases: synthesis, characterization and bio-evaluation. Int J Adv Res 3:563–572

65. Noha AEE, Safa MA, Hassan AF, Abdelaziz HK, Mohamed E, Hesham AH (2017) Green synthesis of graphene from recycled PET bottle wastes for use in the adsorption of dyes in aqueous solution. Ecotoxicol Environ Saf 145:57–68

66. Sogias IA, Khutoryanskiy VV, Williams AC (2010) Exploring the factors affecting the solubility of chitosan in water. Macromol Chem Phys 211:426–433

67. Elkady MF, Mohamed H, Reham A (2015) Equilibrim and kinetics behavior of oil spill process onto synthesized nano-activated carbon. Nano-technol Environ Aspects 3:21–30

68. Asadpour R, Sapari NB, Tuan ZZ, Jusoh H, Riahi A, Uka OK (2013) Review paper application of sorbent materials in oil spill management: a review. Caspian J Appl Sci 2:46–58

69. Sayiter Y (2017) Kinetic and isotherm analysis of Cu (II) adsorption onto almond shell (prunus dulcis). ECOL CHEM ENG S 24:87–106

70. IR-Spectroscopy https://chem.pg.edu.pl

71. Mun GA, Nurkeeva ZS, Dergunov SA, Nama IK, Maimakov TP, Shaikhutdinov EM, Lee SC, Park K (2008) Studies on graft copolymerization of 2- hydroxyethyl acrylate onto chitosan. React Funct Polym 68:389–395

72. Pawlak A, Mucha M (2003) Thermo gravimetric and FTIR studies of chitosan blends. Thermochim Acta 396:153–166

73. Mohy Eldin MS, Omer AM, Hashem AI, Tamer TM (2015) Preparation, characterization and antimicrobial evaluation of novel cinnamyl chitosan Schiff base. Int J Adv Res 3:741–755

74. Chen M, Jiang W, Wang F, Shen P, Ma P, Gu J, Li F (2013) Synthesis of highly hydrophobic floating magnetic polymer nanocomposites for the removal of oils from water surface. Appl Surf Sci 286:249–256

75. Aboulhadeed S (2016) MSc; Development of polymeric composite materials for oil spill removal 1–150

76. Jintao W, Yian Zh, Aiqin W (2014) Kinetic and thermodynamic studies on the removal of oil from water using super hydrophobic kapok fiber. Water Environ Res 86:360–365

77. Nacera Y, Aicha B (2006) Equilibrium and kinetic modelling of methylene blue biosorption by pretreated dead strep tomyces rimosus: effect of temperature. Chem Eng J 119:121–125

78. Zhang J, Wang Q, Wang A (2007) Synthesis and characterization of chitosang- poly (acrylic acid)/ attapuligate super sorbent composits. Carbohydr Polym 68:367–374

79. Elanchezhiyan SSD, Sivasurian N, Meenakshi S (2014) Recovery of oil from oil-in-water emulsion using biopolymers by adsorptive method. Int J Biol Macromol 70:399–407

80. Nwadiogbu JO, Ajiwe VIE, Okoye PAC (2015) Removal of crude oil from aqueous medium by sorption on hydrophobic corncobs: equilibrium and kinetic studies. J Taibah Univ Sci 10:56–63

81. Khaled O, Mona EL-S, Mohamed YEL-K (2011) Treatment of oil–water emulsions by adsorption onto activated carbon, bentonite and deposited carbon. Egypt J Petrol 20:9–15

82. Lin J, Shang Y, Ding B, Yang J, Yu J, Al-deyab SS (2012) Nano porous polystyrene fibers for oil spill cleanup. Mar Pollut Bull 64:347–352

83. Duong HTT, Burford RP (2005) Effect of foam density, oil viscosity, and temperature on oil sorption behavior of polyurethane. J Appl Polym Sci 99:360–367

Publisher's Note Springer Nature remains neutral with regard to jurisdictional claims in published maps and institutional affiliations.

Authors and Affiliations

Bassant Yousry Eweida[1] · Ahmed Mohamed Omer[2] · Tamer Mahmoud Tamer[2] · Hesham Abd-Elfatah Mohamed Soliman[3] · Ahmed Amin Zaatot[4] · Mohamed Samir Mohy-Eldin[2]

[1]   Modeling and Simulation Department, Advanced Technology and New Materials Research Institute (ATNMRI), City of Scientific Research and Technological Applications (SRTA-City), New Borg El-Arab City, Alexandria 21934, Egypt

[2]   Polymer Materials Research Department, Advanced Technology and New Materials Research Institute (ATNMRI), City of Scientific Research and Technological Applications (SRTA-City), New Borg El-Arab City, Alexandria 21934, Egypt

[3]   Nanotechnology and New Composite Materials Department Advanced Technology and New Materials Research Institute (ATNMRI), City of Scientific Research and Technological Applications (SRTA-City), New Borg El-Arab City, Alexandria 21934, Egypt

[4]   Chemical Engineering Department, Faculty of Engineering, Alexandria University, Alexandria, Egypt